

Synaptically Activated Calcium Responses in Dendrites of Hippocampal Oriens-Alveus Interneurons

CHRISTINE E. GEE, GAVIN WOODHALL, AND JEAN-CLAUDE LACAILLE

Centre de Recherche en Sciences Neurologiques, Département de Physiologie, Université de Montréal, Montreal, Quebec H3C 3J7, Canada

Received 13 June 2000; accepted in final form 21 December 2000

Gee, Christine E., Gavin Woodhall, and Jean-Claude Lacaille. Synaptically activated calcium responses in dendrites of hippocampal oriens-alveus interneurons. *J Neurophysiol* 85: 1603–1613, 2001. Activation of metabotropic glutamate receptors (mGluRs) by agonists increases intracellular calcium levels ($[Ca^{2+}]_i$) in interneurons of stratum oriens/alveus (OA) of the hippocampus. We examined the mechanisms that contribute to dendritic Ca^{2+} increases in these interneurons during agonist activation of mGluRs and during synaptically evoked burst discharges, using simultaneous whole cell recordings and confocal Ca^{2+} imaging in rat hippocampal slices. First, we found that the group I/II mGluR agonist 1S,3R-1-aminocyclopentane-1,3-dicarboxylic acid (ACPD; 100 μ M) increased dendritic $[Ca^{2+}]_i$ and depolarized OA interneurons. Dendritic Ca^{2+} responses were correlated with membrane depolarizations, but Ca^{2+} responses induced by ACPD were larger in amplitude than those elicited by equivalent somatic depolarization. Next, we used linescans to measure changes in dendritic $[Ca^{2+}]_i$ during synaptically evoked burst discharges and somatically elicited repetitive firing in disinhibited slices. Dendritic Ca^{2+} signals and electrophysiological responses were stable over repeated trials. Peak Ca^{2+} responses were linearly related to number and frequency of action potentials in burst discharges for both synaptic and somatic stimulation, but the slope of the relationship was steeper for responses evoked somatically. Synaptically evoked $[Ca^{2+}]_i$ rises and excitatory postsynaptic potentials were abolished by antagonists of ionotropic glutamate receptors. The group I/II mGluR antagonist S- α -methyl-4-carboxyphenylglycine (500 μ M) produced a significant partial reduction of synaptically evoked dendritic Ca^{2+} responses. The mGluR antagonist did not affect synaptically evoked burst discharges and did not reduce either Ca^{2+} responses or burst discharges evoked somatically. Therefore ionotropic glutamate receptors appear necessary for synaptically evoked dendritic Ca^{2+} responses, and group I/II mGluRs may contribute partially to these responses. Dendritic $[Ca^{2+}]_i$ rises mediated by both ionotropic and metabotropic glutamate receptors may be important for synaptic plasticity and the selective vulnerability to excitotoxicity of OA interneurons.

INTRODUCTION

In neurons, increasing concentrations of intracellular calcium ($[Ca^{2+}]_i$) mediates processes ranging from presynaptic transmitter release to modification of protein phosphorylation and gene expression (for review see Ghosh and Greenberg 1995). The excitatory neurotransmitter glutamate increases neuronal $[Ca^{2+}]_i$ by a number of mechanisms, including influx

through calcium-permeable ionotropic glutamate receptors (iGluRs), influx through voltage-dependent Ca^{2+} channels, and release from internal stores via activation of metabotropic glutamate receptors (mGluRs) (Berridge 1998; Ghosh and Greenberg 1995). Very high $[Ca^{2+}]_i$ may be induced by excessive glutamatergic stimulation, as during seizure activity, and is toxic to cells (Choi 1994). In temporal lobe epilepsy, principal cells of the hippocampus are lost as a result of such glutamate-mediated excitotoxicity (Dingledine et al. 1990; Meldrum 1995). Gamma-aminobutyric acid-containing interneurons of the hippocampus provide crucial inhibition of projection cells and control their excitability (for review see Freund and Buzsáki 1996). In models of epilepsy, some interneurons of the hippocampus are lesioned in addition to projection cells (Sloviter 1987). In the CA1 region, interneurons in stratum oriens/alveus (OA) and stratum pyramidale are particularly sensitive and are lesioned preferentially in the kainate model of epilepsy (Best et al. 1993; Morin et al. 1998). The mechanism responsible for the specific loss of these interneurons remains unknown.

In models of epilepsy and ischemia, activation of group I mGluRs enhances neurotoxic mechanisms, whereas activation of the group II/III mGluRs has a neuroprotective role (see Nicoletti et al. 1996). In the hippocampus, group II/III mGluRs are largely confined to axons and terminals, whereas the group I mGluRs are situated peri- and extrasynaptically on dendrites of hippocampal neurons (Luján et al. 1996; Shigemoto et al. 1997). Microapplication of glutamate induces mGluR-mediated somatic $[Ca^{2+}]_i$ oscillations in OA interneurons, but not in interneurons of stratum radiatum/lacunosum-moleculare (Carmant et al. 1997). In addition, application of the group I/II mGluR agonist 1S,3R-1-aminocyclopentane-1,3-dicarboxylic acid (ACPD) evokes oscillations of membrane potential and $[Ca^{2+}]_i$ in OA interneurons through activation of voltage-dependent Ca^{2+} channels and Ca^{2+} release from intracellular stores but has little or no effect on stratum radiatum/lacunosum-moleculare interneurons (Woodhall et al. 1999). The presence of these mGluR and Ca^{2+} -mediated mechanisms specifically in OA interneurons raises the possibility that group I/II mGluR activation may be involved in the selective vulnerability of OA interneurons to excitotoxicity. In addition, mGluRs may contribute to synaptic plasticity in OA interneurons as

Address for reprint requests: J.-C. Lacaille, Département de Physiologie, Université de Montréal, c.p. 6128 succursale Centre-ville, Montreal, Quebec H3C 3J7, Canada (E-mail: lacailj@ere.umontreal.ca).

The costs of publication of this article were defrayed in part by the payment of page charges. The article must therefore be hereby marked "advertisement" in accordance with 18 U.S.C. Section 1734 solely to indicate this fact.

long-term potentiation of excitatory synapses, dependent on mGluR activation, has been reported in these neurons (Ouardouz and Lacaille 1995; Perez et al. 2000; but see Maccaferri and McBain 1996). However, if mGluR activation plays a role in excitotoxicity or synaptic plasticity in OA interneurons, then mGluRs should be activated during synaptic transmission and contribute to rises in $[Ca^{2+}]_i$. To address this question, we synaptically evoked epileptiform discharges in OA interneurons from disinhibited rat hippocampal slices and recorded whole cell current-clamp responses while simultaneously monitoring changes in dendritic $[Ca^{2+}]_i$ with confocal microscopy. Some of these data were published in abstract form (Gee et al. 1998).

METHODS

Slice preparation

Transverse hippocampal slices were prepared from young (13–19 day) male Sprague-Dawley rats using similar procedures as Woodhall et al. (1999). The rats were anesthetized with halothane and decapitated, and the brains were rapidly dissected in cold (5°C), oxygenated (95% O₂-5% CO₂) solution containing (in mM) 120 choline-Cl, 2.5 KCl, 26 NaHCO₃, 1.25 NaH₂PO₄, 8 MgSO₄, 10 glucose, and 0.4 L-ascorbic acid, pH 7.35–7.4, ~305 mOsm. Blocks of brain containing the hippocampus were affixed with cyanoacrylate to a vibratome stage and cut into 300- μ m-thick slices. A cut was made to remove the CA3 region from the hippocampus. Slices were transferred to artificial cerebrospinal fluid (ACSF; in mM: 124 NaCl, 2.5 KCl, 2 CaCl₂, 26 NaHCO₃, 1.25 NaH₂PO₄, 2 MgSO₄, 10 glucose, 0.4 L-ascorbic acid, and 4 myo-inositol, pH 7.35–7.4, ~305 mOsm) saturated with 95% O₂-5% CO₂ at room temperature (22–24°C). Slices were allowed to recover for at least 1 h before use.

Electrophysiology

Slices were transferred to a recording chamber attached to the stage of an upright laser scanning confocal microscope (Olympus BH5, BioRad MRC-600, Mississauga, Ontario, Canada). The chamber was perfused with oxygenated ACSF (17–19°C, 1–3 ml/min). Patch pipettes were pulled from borosilicate glass (1 mm OD, A-M Systems, Everett, WA) and filled with 145 mM K-methylsulfate, 1 mM MgCl₂, 8 mM NaCl, 2 mM ATP, 0.4 mM GTP, 10 mM HEPES, 1 mM EGTA, 0.15% biocytin, and 10–20 μ M calcium green I or Oregon green BAPTA-I (Molecular Probes, Eugene, OR), titrated with KOH to pH 7.2–7.25, and adjusted to 275–285 mOsm (electrode resistance 4–8 M Ω). In some experiments, the electrodes were filled with the Ca²⁺ indicator and (in mM) 100 Cs-gluconate, 10 CsCl, 10 NaCl, 2 ATP, 0.4 GTP, 1 EGTA, 10 HEPES, 20 QX-314 bromide, 0.15% biocytin, titrated to 7.2–7.25 with acetic acid, and adjusted to 275–285 mOsm (4–8 M Ω). Whole cell patch-clamp recordings were obtained, under visual control using a long working-distance water-immersion objective (Olympus WPlanFL \times 40 UV, 0.7 numerical aperture, 3.1 mm working distance), from CA1 OA interneurons, with horizontally oriented primary dendrites and somata near the oriens/alveus border, as previously described (Woodhall et al. 1999). Changes in membrane voltage were monitored using an Axoclamp-2B amplifier (Axon Instruments, Foster City, CA) in bridge mode. Signals were digitized at 22 kHz and recorded to videotape. In addition, signals were filtered at 1 kHz, digitized at 2 kHz (TL-1, Axon Instruments), stored on a PC, and analyzed using pClamp software (Axon Instruments). The bridge balance was monitored and adjusted using the bridge circuit. Cells with an initial resting membrane potential more negative than –45 mV, overshooting action potentials, and an input resistance >200 M Ω were accepted. To control for the effects of membrane potential on input resistance and to reduce spontaneous action potentials, current

(approximately \pm 50 pA) was injected to set the membrane potential near –60 to –65 mV. At this membrane potential, the input resistance of the OA interneurons was 403 \pm 27 M Ω (mean \pm SE, n = 37).

A monopolar tungsten microelectrode was positioned in stratum radiatum (or occasionally in the alveus) to synaptically activate OA interneurons via their excitatory input from CA1 pyramidal cells (e.g., Blasco-Ibanez and Freund 1995; Lacaille et al. 1987). OA interneurons were also activated by somatic depolarizing current injection via the recording electrode.

Calcium imaging

After obtaining the whole cell configuration, at least 20 min were allowed for intracellular diffusion of the fluorophore. The fluorophore was excited using a 488-nm argon laser attenuated to 1% of the maximum power. Emission was detected through a long-pass filter (cutoff 515 nm) and recorded to a PC using the MPL software (BioRad). The confocal aperture was opened fully. Linescans were taken from dendrites approximately 100–150 μ m from the soma at a rate of 12 ms per line for a total scan time of 6.144 s. Alternatively, time lapse images were collected at 0.2 Hz. The images were analyzed off-line using Cfocal and Bfocal software (provided by M. Charlton, University of Toronto, Toronto, Ontario, Canada). For linescans, the fluorescence intensity (F_{line}) of a line was averaged for a delimited region of interest representing a section of the dendrite. Changes in fluorescence were calculated for each line relative to the averaged baseline fluorescence prior to stimulation (F_{rest}) and expressed as

$$\% \Delta F/F = [(F_{line} - F_{rest})/F_{rest}] \times 100$$

The values were then processed with a low-pass digital filter to remove fast transients (SigmaPlot, SPSS Chicago, IL, corner frequency 10 Hz, e.g., Fig. 3), and the peak calcium response was determined for each linescan. Since Ca²⁺ responses were often fractionated and consisting of multiple peaks (ex. Fig. 4), the area under the calcium response was calculated until either the return to baseline or the end of the linescan (whichever occurred 1st, time interval 0.9–5.2 s following the stimulation) from the filtered waveforms using a trapezoidal rule-based algorithm (SigmaPlot). For each time lapse image, the average fluorescence was measured for a region of interest of the dendrite; the change in fluorescence was then calculated for each image relative to the average baseline fluorescence of the prestimulation images using the above formula. The area under the response was then calculated from the start of the response until a return to baseline up to a maximum 7-min period using the same algorithm as for the linescans.

Linescans were initiated by a digital trigger pulse. After a 1-s delay, synaptic stimulation was applied via the tungsten electrode, or somatic current injection was applied via the recording electrode. To compensate for small variations in the start time of the linescans, electrophysiological and Ca²⁺ responses were temporally aligned by eye. This correction and the relatively slow scan time used (12 ms per line) prevented a more precise temporal analysis of the Ca²⁺ and voltage responses.

Pharmacology

Experiments were carried out in the presence of 20 μ M bicuculline methiodide to block GABA_A-mediated inhibition. In some experiments, (\pm)-2-amino-5-phosphopentanoic acid (APV, 200 μ M) and 6-cyano-7-nitroquinoxaline-2,3-dione (CNQX, 40 μ M) were used to block ionotropic glutamate receptor (iGluR) activation. During experiments with the mGluR agonist ACPD, tetrodotoxin (TTX, 0.5 μ M) was used to prevent action potentials and indirect effects of the agonist. (S)- α -methyl-4-carboxyphenylglycine (S-MCPG) was used to antagonize mGluRs. ACPD and MCPG were purchased from Tocris-Cookson (Ballwin, MO). APV and CNQX were purchased

from RBI (Nantick, MA). K-methylsulphate and choline chloride were purchased from ICN (Costa Mesa, CA). L-Ascorbic acid was purchased from Fisher (Ottawa, Ontario, Canada). Other chemicals were purchased from Sigma (Oakville, Ontario, Canada).

Histology

After recording, the slices containing biocytin-filled cells were transferred to a freshly prepared solution of 4% paraformaldehyde in 0.1 M phosphate buffer and fixed overnight at 4°C. Slices were washed and stored in 0.1 M phosphate buffer for up to 2 wk then embedded in agarose and resectioned at 50–80 μm with a vibratome. The sections were then processed using the Vectastain ABC kit (Vector Laboratories, Burlingame, CA) followed by nickel-intensification as previously described (Woodhall et al. 1999). Sections were mounted with D.P.X. mounting medium (Electron Microscopy Sciences, Ft. Washington, PA) and examined under a light microscope.

Statistics

Data are expressed as means \pm SE. Data were tested for normality, and equal variance and appropriate parametric or nonparametric tests were applied using SigmaStat statistical software (SPSS). Significance level was set at $P < 0.05$.

RESULTS

Intradendritic Ca^{2+} increases mediated by mGluR activation

Activating mGluRs by bath application of the group I/II agonist (1S,3R)-ACPD increases intrasomatic Ca^{2+} and causes depolarization of OA interneurons (McBain et al. 1994; Woodhall et al. 1999). To assess whether similar Ca^{2+} responses are produced in dendrites, we applied ACPD (100 μM) in the presence of TTX (0.5 μM) to block action potentials and possible indirect effects. Confocal images were collected at 0.2 Hz from dendrites of OA interneurons filled with the Ca^{2+} indicator oregon green BAPTA-I. In the presence of ACPD, 11 of 13 cells depolarized (range, 4.0–31.3 mV; mean depolarization, 13.7 ± 2.2 mV), and 2 cells showed no change in membrane potential. In these experiments, the mean membrane potential prior to ACPD application was -60.2 ± 0.6 mV. Dendritic $[\text{Ca}^{2+}]_i$ increased in the cells that depolarized (mean peak Ca^{2+} response $57.7 \pm 14.9\% \Delta F/F$, $n = 11$) and did not change in the cells that did not depolarize. Figure 1 shows a typical response from one of the cells that depolarized and showed an increase in dendritic $[\text{Ca}^{2+}]_i$ in the presence of ACPD. We occasionally saw oscillatory responses to bath application of ACPD (see Woodhall et al. 1999). Cell input resistance was monitored, with hyperpolarizing current pulses, in three cells during ACPD responses. It decreased in two cells (by 92 and 44%), and increased by 6% in the other.

We examined the relationship between dendritic Ca^{2+} responses and depolarizations induced by ACPD. The peak amplitude of ACPD-induced dendritic Ca^{2+} rises and depolarizations were significantly correlated ($r^2 = 1.453$, $P = 0.023$, $n = 11$, Fig. 2A). ACPD-induced Ca^{2+} and depolarizing responses were also correlated in time with an average latency to peak of 338 ± 30 and 349 ± 31 s, respectively, following the onset of ACPD ($r^2 = 0.826$, $P < 0.001$, $n = 11$, Fig. 2B). This latency to peak was consistent with the time required for solution exchange in our perfusion system. We used somatic current injections to evoke dendritic Ca^{2+} responses of nonsynaptic origin. The peak amplitude of these dendritic Ca^{2+} responses

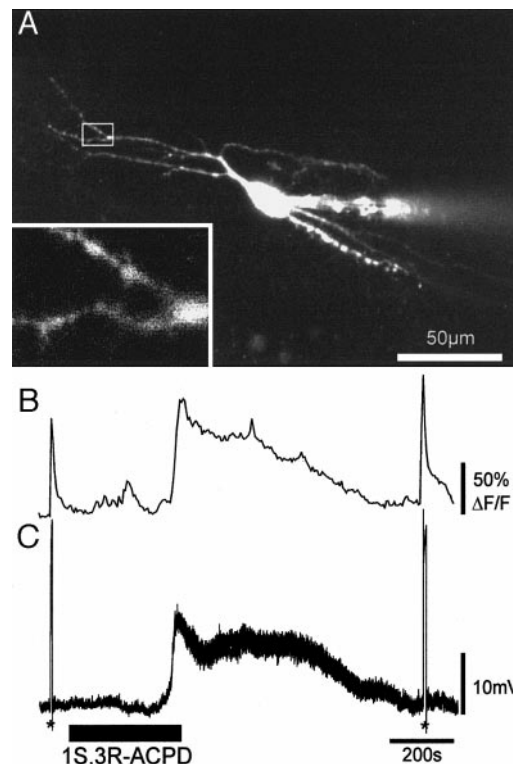


FIG. 1. Effects of 100 μM 1S,3R-1-aminocyclopentane-1,3-dicarboxylic acid (ACPD) on dendritic Ca^{2+} levels and membrane potential of an oriens/alveus (OA) interneuron in 0.5 μM tetrodotoxin (TTX). *A*: projected confocal image from a z -series (5- μm steps) of an OA interneuron filled with oregon green BAPTA-I. The dendritic region of interest is indicated by the white box and is shown at high magnification in the *inset*. *B* and *C*: bath application of ACPD increased dendritic $[\text{Ca}^{2+}]_i$ in the region of interest (*B*) and depolarized the OA interneuron (*C*) with an increase in baseline noise. Depolarizing current was injected via the patch pipette at the times indicated by the asterisks.

was significantly correlated with the somatic depolarizations ($r^2 = 0.193$, $P = 0.022$, $n = 27$ observations from 11 dendrites, Fig. 2A). The slope of the linear regression for the Ca^{2+} -voltage relation was less for somatic depolarizations than for ACPD responses (Fig. 2). The soma depolarizations required to evoke dendritic Ca^{2+} responses similar to those induced by ACPD ($54.3 \pm 12.8\% \Delta F/F$, $n = 11$) were larger (27.8 ± 2.8 mV, $n = 11$) than the ACPD-induced depolarizations (Fig. 2A). We also used somatic depolarizations as control Ca^{2+} responses before and after ACPD responses (Fig. 1). Ca^{2+} responses ($82.0 \pm 25.9\% \Delta F/F$) evoked by soma depolarizations (29.0 ± 3.1 mV) were not significantly different after the ACPD application ($P = 0.22$, $n = 10$, t -test).

Biocytin-labeled cells that responded to ACPD had horizontally oriented cell bodies with dendrites confined to stratum oriens/alveus (9/10 cells), or that also crossed stratum pyramidale and entered strata radiatum/lacunosum-moleculare (1/10 cells). The axons of these cells were seen exclusively in stratum oriens/alveus (2/5 cells), in strata oriens/alveus, radiatum and lacunosum-moleculare (1/5 cells), or in radiatum and lacunosum-moleculare (2/5 cells). The biocytin-labeled ACPD-insensitive cells had horizontally oriented dendrites in stratum oriens/alveus (1/2 cells) or also dendrites that crossed stratum pyramidale and entered strata radiatum/lacunosum-moleculare (1/2 cells). The axons of the nonresponsive cells projected to stratum oriens/alveus (1/2 cells) or to strata pyramidale/radia-

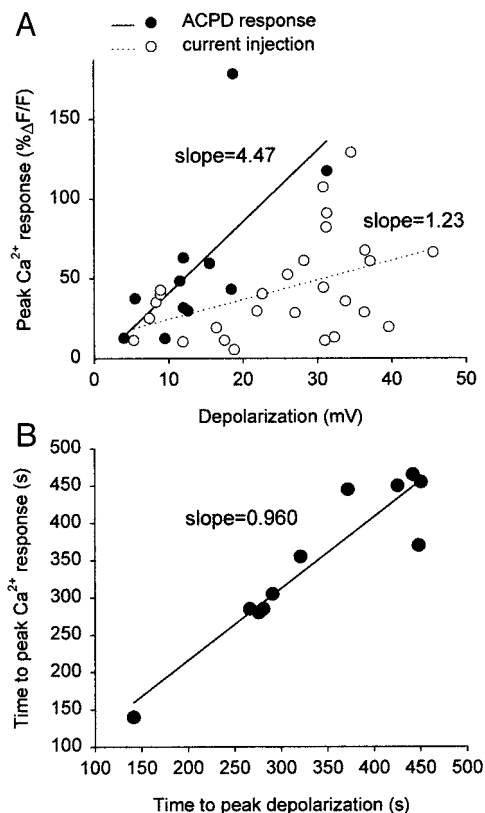


FIG. 2. Relationship between dendritic Ca^{2+} response and soma depolarization. *A*: graph of the peak amplitude of dendritic Ca^{2+} rises vs. somatic depolarization induced by ACPD (●, —, $n = 11$), showing the significant correlation between Ca^{2+} response and depolarization. There was also a significant correlation between dendritic Ca^{2+} rises and depolarizations induced by soma current injections (○, ···, $n = 27$). However, the slope of the linear regression was less for somatic than ACPD-induced responses. *B*: graph of the time-to-peak of Ca^{2+} responses vs. time-to-peak of depolarizations induced by ACPD, showing the significant temporal correlation between the 2 components of ACPD responses ($n = 11$).

tum (1/2 cells). Thus no clear relationship was observed between the morphology of OA interneurons and the electrophysiological and/or Ca^{2+} responses induced by ACPD.

Intradendritic Ca^{2+} responses evoked by synaptic activation

To examine synaptically evoked responses, we combined current-clamp recordings of excitatory postsynaptic potentials (EPSPs) and burst discharges in OA interneurons held at membrane potentials near -60 to -65 mV, with imaging of dendritic Ca^{2+} responses in linescan mode. OA interneurons were activated polysynaptically, with a tungsten electrode placed in stratum radiatum in the presence of $20 \mu\text{M}$ bicuculline. Large epileptiform EPSPs triggering multiple action potentials were recorded at the soma in response to single stimuli (20 – $130 \mu\text{A}$ for $500 \mu\text{s}$) in stratum radiatum (Fig. 3*D*). When the stimulating electrode was placed in the alveus, smaller but qualitatively similar responses were recorded in OA interneurons (not shown). Dendritic Ca^{2+} increased during the synaptically evoked burst discharge (Fig. 3*D*). Dendritic $[\text{Ca}^{2+}]_i$ rose rapidly during the responses and decayed slowly over seconds. All linescans were filtered to remove fast transients before measuring response parameters (see METHODS). The sample Ca^{2+} responses shown in Fig. 3, *D*–*F*, show both filtered and

unfiltered traces. Whereas the filtering reduced the peak amplitude of Ca^{2+} responses by $8.7 \pm 7.1\% \Delta F/F$ ($n = 7$ cells randomly selected), it did not affect the time-to-peak or the ability to resolve smaller peaks associated with individual action potentials. The filtering was useful in reducing background fluctuations. Ca^{2+} responses associated with individual action potentials were more clearly resolved when the interspike interval exceeded about 30 ms (e.g., Fig. 3, *E* and *F*) but were not observed in all cells (e.g., Fig. 8).

In 22 of 30 cells, Ca^{2+} levels were stable during the prestimulus baseline period (e.g., Fig. 3, *E* and *F*). In 17 of these 22 cells, Ca^{2+} responses returned to baseline levels before the end of the linescans (within 5.2 s from the time of stimulation). In the remaining 8 of 30 cells, fluorescence declined during the prestimulus period (e.g., Figs. 3*D* and 4), possibly due to bleaching of the dye. This decline was nonlinear and was not corrected. In five of these eight cells, Ca^{2+} responses returned to baseline levels during the linescans (e.g., Fig. 4).

To distinguish between action potential and synaptically generated dendritic Ca^{2+} responses, changes in dendritic $[\text{Ca}^{2+}]_i$ were monitored while a similar number of action potentials was generated by somatic current injection (Fig. 4, *A1* and *B1*). During these experiments, exposure to the laser was kept to a minimum to avoid phototoxic damage to the cells. For each condition, two linescans, one during synaptic stimulation and one during somatic activation, were collected at the same dendritic location and usually at 1- to 2-min intervals, for a total of six to eight linescans per cell. Fluorescence levels usually returned to baseline during the 1- to 2-min intervals. Occasionally, changes in baseline fluorescence occurred between longer intervals. To control for the possibility of time-dependent changes in either synaptically or somatically evoked responses, we collected several linescans over longer intervals (Fig. 4). The mean peak Ca^{2+} response and the mean area under the Ca^{2+} response were not significantly different during 75 min of recording for both synaptic stimulation (peak Ca^{2+} , $F = 0.197$, $P = 0.823$; area under Ca^{2+} response, $F = 0.654$, $P = 0.534$, $n = 7$ cells) and somatic activation (peak Ca^{2+} , $F = 0.284$, $P = 0.764$; area under Ca^{2+} response, $F = 0.30$, $P = 0.971$, $n = 3$ cells; Fig. 4, 1-way ANOVAs). Similarly, the number of action potentials were stable over time whether evoked synaptically ($H = 0.494$, $P = 0.781$; $n = 7$ cells) or somatically ($H = 0.935$, $P = 0.686$; $n = 3$ cells; Fig. 4, Kruskal-Wallis).

We examined the relationships between peak Ca^{2+} response and burst characteristics for both synaptically and somatically evoked responses. Peak Ca^{2+} responses were plotted against the number of action potentials and mean spike frequency for the complete data set with both stimulation types (Fig. 5). Peak Ca^{2+} response was linearly related to the electrophysiological measure with either synaptic stimulation (number of action potentials: $r^2 = 0.153$, $P = 0.007$; action potential frequency: $r^2 = 0.134$, $P = 0.014$) or somatic stimulation (number of action potentials: $r^2 = 0.215$, $P = 0.009$; action potential frequency: $r^2 = 0.234$, $P = 0.006$). However, the slope of the relationships between peak Ca^{2+} response and the characteristics of the underlying bursts of action potentials was steeper for somatically than synaptically evoked responses (see Fig. 5, *A* and *B*), suggesting some differences between the two types

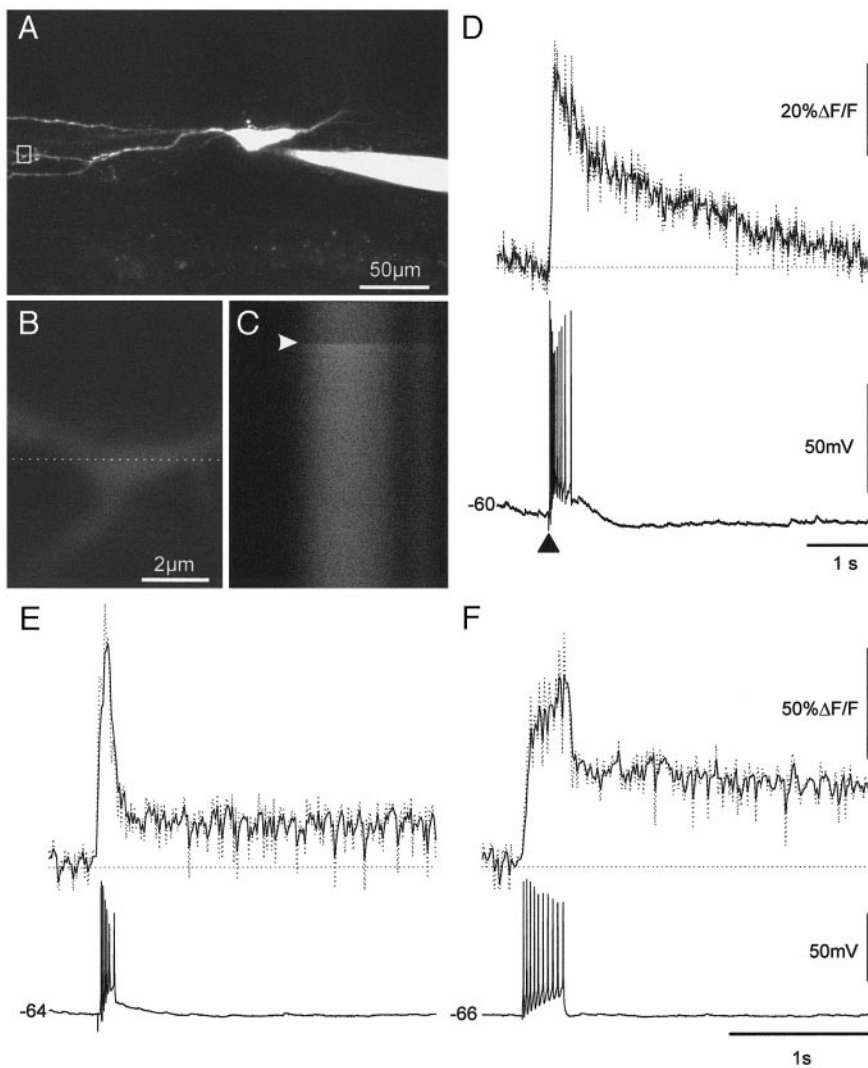


FIG. 3. Synaptically evoked dendritic Ca^{2+} responses in OA interneurons during stimulation of stratum radiatum in bicuculline ($20 \mu\text{M}$). *A*: projected confocal image from a z -series ($5\text{-}\mu\text{m}$ steps) of an OA interneuron filled with oregon green BAPTA-1 with the dendritic region of interest indicated by the white box. *B*: the region of interest is shown at higher magnification, and the repetitively scanned line is indicated by the dashed white line. *C*: a complete linescan (512 lines) during which a single stimulus (indicated by arrowhead) was applied in stratum radiatum 1 s after starting the scan ($t = 0$ at top; $t = 6.144$ s at bottom). *D*: the bottom trace shows the synaptic depolarization and burst discharge recorded at the soma. The top traces show the simultaneous Ca^{2+} response measured from *C*. The dotted line is the unfiltered trace, and the solid line is the filtered trace. *E* and *F*: 2 linescans (top traces) taken from a different cell showing both filtered (solid) and unfiltered (dotted) Ca^{2+} responses and the corresponding electrophysiological recordings (bottom traces) for synaptically (*E*) and somatically (*F*) evoked responses. The filtering did not prevent the detection of Ca^{2+} signals associated with individual action potentials. However, with interspike intervals shorter than approximately 30 ms (compare *E* and *F*), Ca^{2+} signals associated with individual action potentials were difficult to detect.

of Ca^{2+} responses. Similar relationships were also found for the area under Ca^{2+} responses (not shown).

EPSPs and dendritic Ca^{2+} responses require iGluR activation

We next examined the role of iGluRs in responses evoked by synaptic and somatic stimulation. Bath application of the *N*-methyl-D-aspartate (NMDA) receptor antagonist APV ($200 \mu\text{M}$) and the α -amino-3-hydroxy-5-methyl-4-isoxazolepropionic acid (AMPA)/kainate receptor antagonist CNQX ($40 \mu\text{M}$) eliminated the electrophysiological and dendritic Ca^{2+} responses evoked by synaptic stimulation (peak Ca^{2+} response, $W = -45.0$, $P = 0.004$; area under Ca^{2+} response, $W = -45.0$, $P = 0.004$; number of action potentials, $W = -36.0$, $P = 0.008$; $n = 9$, Wilcoxon signed rank test; Fig. 6). These effects were reversible following wash out of CNQX/APV. Peak Ca^{2+} responses recovered to $74.4 \pm 7.4\%$ of control, area under Ca^{2+} responses to $119.5 \pm 7.3\%$ of control, and number of spikes to $94.9 \pm 17.4\%$ of control ($n = 3$). APV and CNQX did not affect either the electrophysiological or dendritic Ca^{2+} responses evoked by somatic activation (peak Ca^{2+} , $t = -0.510$, $P =$

0.626 ; area under Ca^{2+} response, $t = -0.275$, $P = 0.826$; number of action potentials, $t = 0.0$, $P = 1.0$, $n = 9$, Student's *t*-test; Fig. 6, *C* and *D*). In the OA interneuron shown in Fig. 6, the stimulating electrode placed in stratum radiatum also elicited an antidromic action potential. The dendritic Ca^{2+} response elicited by this action potential was not blocked by the antagonists. This was the only cell in which antidromic action potentials were elicited by the synaptic stimulation. Similar Ca^{2+} responses to individual spontaneous action potentials were seen in other cells (e.g., Fig. 4). These results indicate that activation of iGluRs is necessary for synaptically evoked burst discharges and dendritic Ca^{2+} responses, but not for responses to somatic activation.

We attempted to visualize intradendritic Ca^{2+} responses to synaptic stimulation using an intracellular patch solution containing cesium and QX-314 to block K^+ and voltage-gated Na^+ channels. In these conditions, mGluR-mediated activation of a Ca^{2+} -dependent nonselective cation current has been observed in CA1 pyramidal cells, in the absence of iGluR activation (Congar et al. 1997). With this protocol, dendritic Ca^{2+} responses were detected during large amplitude and long duration EPSPs elicited by single stimuli or 100-Hz/1-s trains.

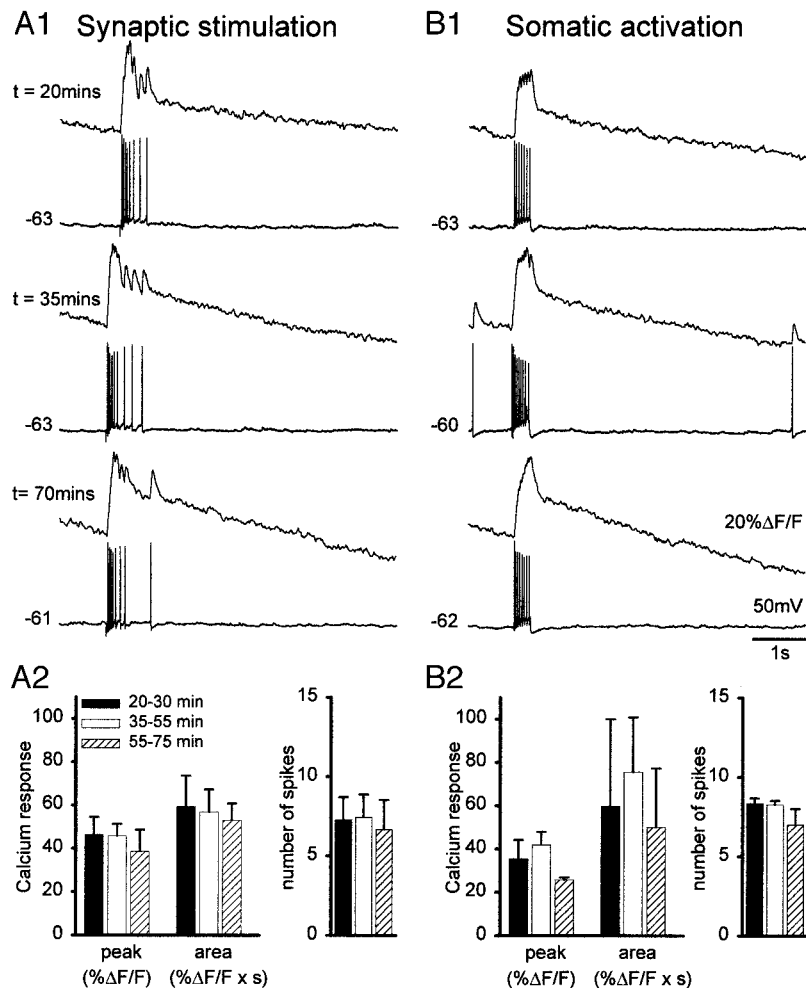


FIG. 4. Stability of electrophysiological and dendritic Ca^{2+} responses evoked by synaptic and somatic stimulation. *A1*: electrophysiological (*bottom trace*) and dendritic Ca^{2+} (*top trace*) responses were evoked by synaptic stimulation at the time points indicated in an interneuron. *B1*: to distinguish synaptically generated Ca^{2+} responses from action potential-evoked Ca^{2+} responses, responses to somatic current injection producing a similar number of action potentials were recorded at the same dendritic location, either 1 min before or after the traces in *A1*. *A2* and *B2*: graphs, for all cells tested, of mean increases in dendritic $[\text{Ca}^{2+}]_i$ and mean number of action potentials evoked by synaptic (*A2*) or somatic activation (*B2*) at different time points, indicating that Ca^{2+} and electrophysiological responses did not significantly change over these long recording intervals.

However, in the presence of APV and CNQX, these dendritic Ca^{2+} signals, as well as EPSPs, were completely abolished (Fig. 7, $n = 11$ cells). Thus in our experimental conditions, no dendritic Ca^{2+} responses were detected in the presence of iGluR antagonists.

mGluR activation contributes to synaptically evoked dendritic Ca^{2+} responses

To determine whether mGluRs contribute to synaptically evoked responses, we examined the effects of the group I/II mGluR antagonist MCPG (500 μM ; $n = 14$ cells). This antagonist required long wash out periods (30–45 min). Therefore the time required to 1) load the cells with the calcium-sensitive dye, 2) obtain synaptically and somatically evoked responses, and 3) record responses following drug application and wash out was longer than 70 min. Dendritic Ca^{2+} responses to somatic activation and synaptic stimulation sometimes deteriorated after the long wash out of MCPG from the slice. Therefore responses were evoked in six cells, first in the presence of MCPG and then in normal ACSF following a 30- to 45-min wash out. In the remaining cells ($n = 11$), responses were obtained first in normal ACSF and then in the presence of MCPG; in some of these cells ($n = 5/11$), a wash out of MCPG was possible. In three cells exposed to MCPG, the linescan intersected two distinct dendritic branches of the same cell. In

two of these cells, MCPG reduced synaptically evoked Ca^{2+} responses to a greater extent in one of the two branches (data not shown). Thus mGluR contributions to synaptically evoked dendritic Ca^{2+} responses appeared spatially localized to certain dendritic sites in certain cells, and consequently responses in both dendrites of these three cells were analyzed as separate observations. The mean peak amplitude and area under the response of synaptically evoked Ca^{2+} responses were significantly reduced in the presence of MCPG (Fig. 8*B1*; peak Ca^{2+} response, $t = 3.69$, $P = 0.002$; area under Ca^{2+} response, $t = 2.543$, $P = 0.022$; paired t -tests, $n = 17$). In the five cases with MCPG wash out, the peak amplitude of synaptically evoked Ca^{2+} responses was significantly reduced to $75.7 \pm 8.4\%$ of control in the presence of MCPG and recovered partially to $82.8 \pm 8.4\%$ of control after wash out. By contrast, MCPG did not significantly affect dendritic Ca^{2+} responses evoked by somatic activation in the same cells (Fig. 8*D1*; peak Ca^{2+} response, $t = 1.708$, $P = 0.119$; area under Ca^{2+} response, $t = 0.820$, $P = 0.44$, $n = 10$; paired t -tests). EPSPs and burst discharges evoked by synaptic stimulation were also not significantly changed in the presence of MCPG (Fig. 8, *A2* and *B2–B4*; number of action potentials, $t = 0.504$, $P = 0.69$; action potential frequency, $t = 1.06$, $P = 0.31$; action potential amplitude, $t = 1.48$, $P = 0.16$; $n = 14$, paired t -tests). Similarly, MCPG did not significantly affect somatically evoked repetitive firing (Fig. 8, *C2* and *D2–D4*; number of action

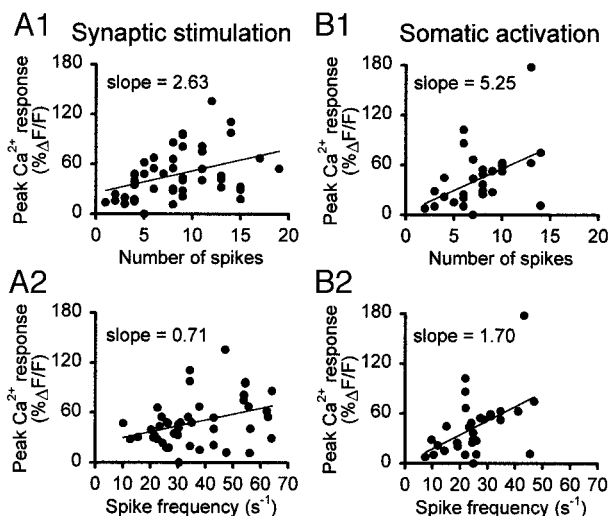


FIG. 5. Relationship between peak Ca^{2+} responses and action potential number and frequency. *A*: graphs of peak Ca^{2+} responses evoked in all cells by synaptic stimulation as a function of number (*A1*) and frequency (*A2*) of action potentials. *B*: similar data for peak Ca^{2+} responses evoked by somatic activation. For both types of stimulation, a significant linear correlation was found between peak Ca^{2+} responses and number or frequency of action potentials in the burst. The slopes of the linear regressions were steeper for somatic than synaptic responses.

potentials, $t = -1.562$, $P = 0.153$; action potential frequency, $t = -1.20$, $P = 0.26$; action potential amplitude, $t = 0.845$, $P = 0.42$; $n = 10$; paired t -tests). These results suggest that mGluRs may contribute in part to dendritic Ca^{2+} responses but not to EPSPs and burst discharges evoked by synaptic stimulation, and they do not contribute to Ca^{2+} responses or repetitive firing evoked by somatic activation.

Biocytin-labeled cells that were responsive to MCPG had horizontally (4/5) or vertically (1/5) oriented cell bodies and horizontally oriented dendrites confined to stratum oriens/alveus. In one cell, the axon projected to stratum lacunosum-moleculare, whereas in the other cells it ramified in strata pyramidale/radiatum and lacunosum-moleculare. Biocytin-labeled cells that showed no effect of MCPG had dendrites confined to oriens/alveus (1/2) or also crossing into strata radiatum/lacunosum-moleculare (1/2). Their axon projected to stratum pyramidale (1/2) or strata pyramidale/radiatum (1/2).

DISCUSSION

In the present study, we found that direct activation of mGluRs with the group I/II agonist ACPD increased dendritic Ca^{2+} levels and depolarized OA interneurons. We also observed that mGluRs may contribute in part to dendritic Ca^{2+} increases during synaptically evoked burst discharges in OA interneurons since the group I/II mGluR antagonist MCPG produced a significant partial reduction of synaptically evoked Ca^{2+} responses, without affecting electrophysiological burst discharges, nor dendritic Ca^{2+} responses elicited by somatic action potentials. Finally, synaptically evoked Ca^{2+} responses were abolished by blocking ionotropic glutamate receptors, suggesting that their co-activation may be necessary for mGluR-mediated Ca^{2+} responses. Thus ionotropic and metabotropic GluRs may jointly contribute to dendritic Ca^{2+} rises during synaptic activity in OA interneurons, which may

be important for Ca^{2+} -mediated synaptic plasticity or excitotoxicity.

Activation of mGluRs by ACPD increases dendritic $[\text{Ca}^{2+}]_i$

The Ca^{2+} response and depolarization of OA interneurons produced by application of ACPD confirms previous findings that ACPD increases $[\text{Ca}^{2+}]_i$ in somata and proximal dendrites (Woodhall et al. 1999) and induces Ca^{2+} -dependent inward currents (McBain et al. 1994) in OA interneurons. Our results extend these findings by demonstrating that $[\text{Ca}^{2+}]_i$ in more distal dendrites also increases in response to ACPD. The effects of ACPD were not mediated indirectly since TTX was used to block action potential-driven synaptic transmission. The ACPD-induced increase in dendritic Ca^{2+} levels and de-

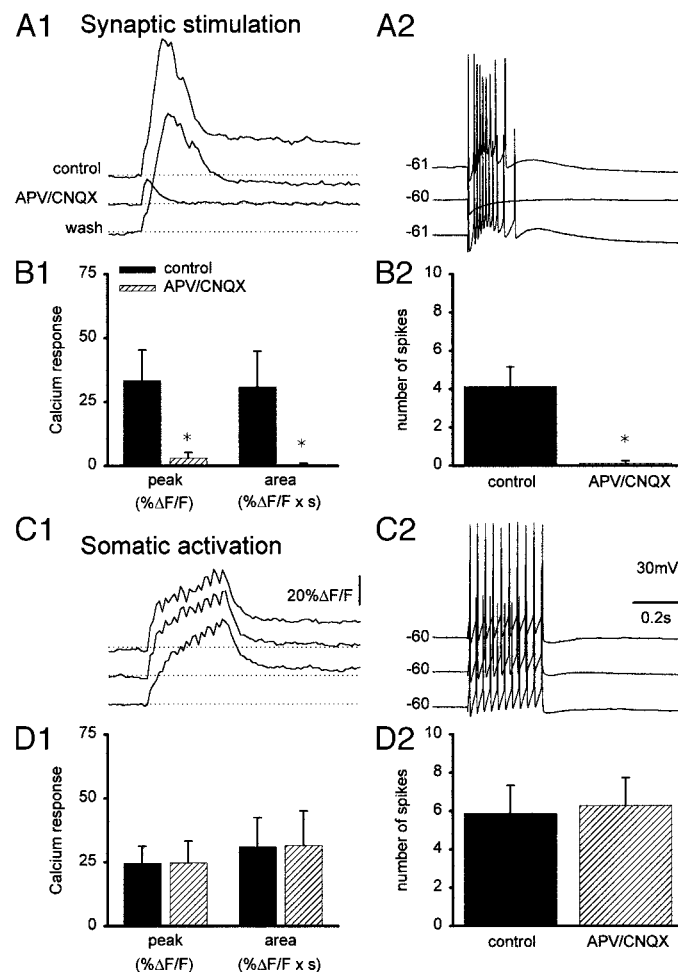


FIG. 6. Block of synaptically evoked dendritic Ca^{2+} responses and excitatory postsynaptic potentials (EPSPs) by ionotropic glutamate receptor antagonists. *A* and *B*: traces taken from a representative cell (*A*) and histograms (*B*) showing mean values of synaptically evoked responses for all cells tested ($n = 6$). In (\pm) -2-amino-5-phosphopentanoic acid (APV; $200 \mu\text{M}$) and 6-cyano-7-nitroquinoxaline-2,3-dione (CNQX; $50 \mu\text{M}$), synaptically evoked dendritic Ca^{2+} responses (*A1* and *B1*) and EPSPs/burst discharges (*A2* and *B2*) were blocked. In the OA interneuron shown, the stimulating electrode placed in stratum radiatum also elicited an antidromic action potential. The dendritic Ca^{2+} response elicited by this action potential was not blocked by the antagonists. *C* and *D*: neither dendritic Ca^{2+} responses (*C1* and *D1*) nor repetitive firing (*C2* and *D2*) elicited by somatic current injection were affected by APV/CNQX. Asterisks indicate groups that are significantly different from control.

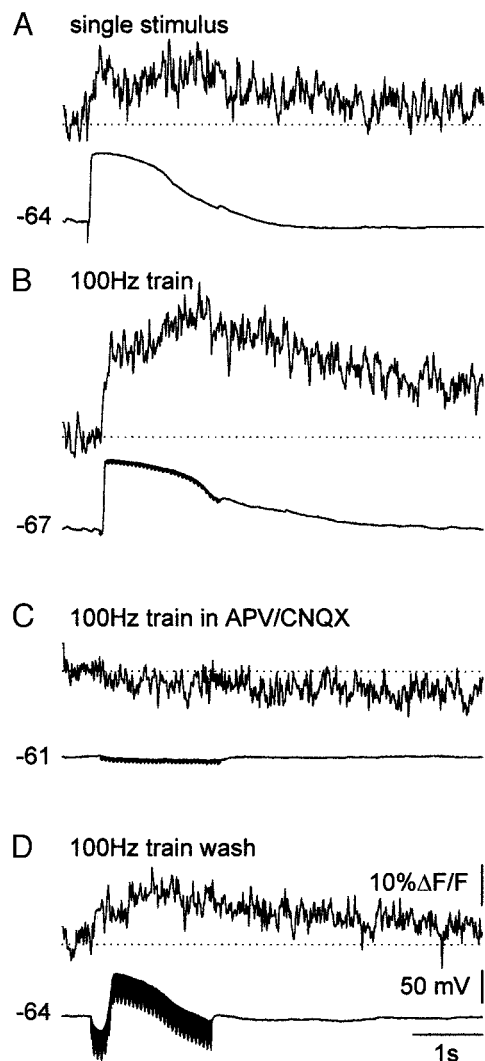


FIG. 7. Dendritic Ca^{2+} responses and EPSPs during blockade of Na^+ and K^+ channels with intracellular QX-314 and Cs^+ . *A* and *B*: traces from a representative cell recorded with an intracellular patch solution containing Cs^+ and QX-314, showing that stimulation with single pulses (*A*) or 1-s/100-Hz trains (*B*) elicited large, long duration EPSPs (*bottom traces*) that were accompanied by dendritic Ca^{2+} rises (*top traces*). *C*: in the presence of 20 μM CNQX and 100 μM APV, both Ca^{2+} and electrophysiological responses were completely abolished. *D*: the effects of CNQX/APV were partially reversible after wash out of the antagonists.

polarization were significantly correlated. However, larger current-evoked somatic depolarizations were required to produce dendritic Ca^{2+} responses similar to those induced by ACPD. Since Ca^{2+} changes were measured in the dendrites, this difference could be due to voltage attenuation of somatic evoked depolarizations from the soma to the dendritic location. Alternatively, ACPD-induced rises in dendritic Ca^{2+} levels may involve other mechanisms in addition to influx through voltage-dependent Ca^{2+} channels, likely through the previously reported mGluR-mediated coupling of voltage-dependent Ca^{2+} channels and Ca^{2+} release from intracellular stores (Woodhall et al. 1999). The dendritic Ca^{2+} responses and somatic depolarizations were temporally correlated in our experiments. However, with the slow acquisition rate of the confocal images we used (0.2 Hz), it was not possible to determine more precisely the temporal relationship between

dendritic Ca^{2+} changes and membrane depolarization (Bianchi et al. 1999).

Postsynaptic group I mGluRs have been localized immunohistochemically to peri- and extra-synaptic regions of dendrites on OA interneurons, with the somatostatin/GABA containing interneurons in OA expressing high levels of mGluR1 α (Baude et al. 1993; Luján et al. 1996). In contrast, group II mGluRs are located presynaptically (Shigemoto et al. 1997). Thus the mGluR responses observed were likely due to direct activation of dendritic postsynaptic group I mGluRs.

Mechanisms of synaptically evoked Ca^{2+} responses

We found that peak dendritic Ca^{2+} responses, evoked either synaptically or somatically, were linearly related to the number and frequency of action potentials in burst discharges, but that the slope of the relationship was steeper for somatic than synaptic responses. This linear relationship between peak Ca^{2+} response and action potential number or frequency may not be

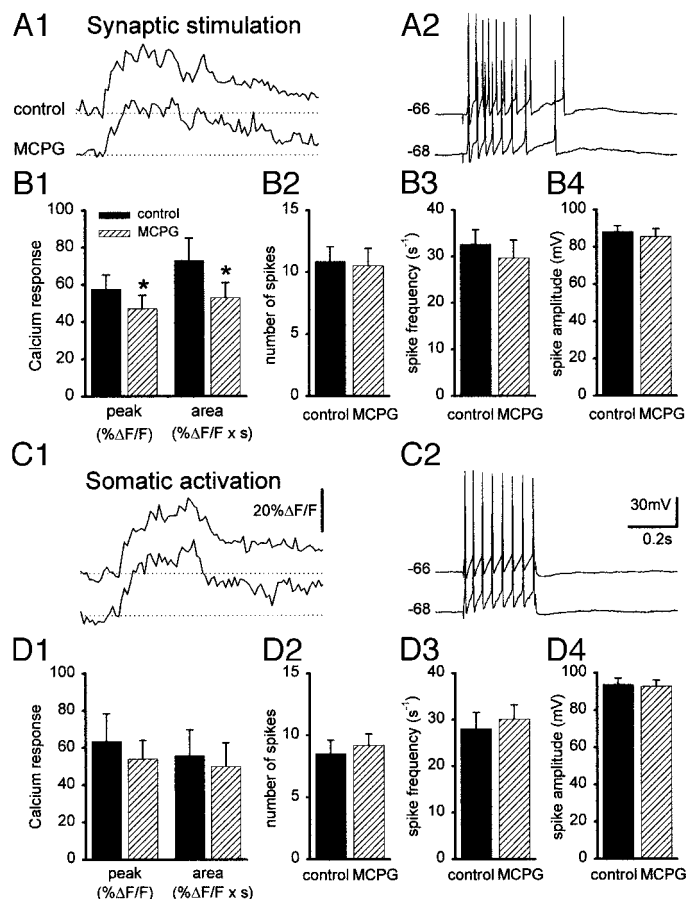


FIG. 8. Significant partial reduction of synaptically evoked dendritic Ca^{2+} responses by the mGluR antagonist (S)- α -methyl-4-carboxyphenylglycine (MCPG; 500 μM). *A* and *B*: example of synaptically evoked responses from a representative cell (*A*) and histograms for all cells tested (*B*) showing that MCPG significantly reduced the amplitude and area under dendritic Ca^{2+} responses (*A1* and *B1*). The number of action potentials evoked by synaptic stimulation did not change in MCPG (*A2* and *B2*). MCPG did not significantly affect either action potential frequency (*B3*) or amplitude (*B4*) during synaptically evoked burst discharges. *C* and *D*: MCPG did not significantly affect Ca^{2+} responses (*C1* and *D1*), nor various parameters of repetitive discharge (*C2* and *D2–D4*) evoked by somatic activation. Asterisks indicate significantly different from control.

absolutely accurate since Ca^{2+} responses were obtained in different cells in these experiments. Still, since most synaptically and somatically evoked responses were recorded in the same cells, these results suggest that different mechanisms may underlie these two types of dendritic Ca^{2+} responses. This difference likely reflects the additional activation of glutamate receptor mechanisms during synaptic responses.

The absence of synaptically evoked Ca^{2+} responses (or EPSPs) in OA interneurons when iGluRs were blocked suggests that synaptically evoked mGluR-mediated Ca^{2+} responses may require co-activation of iGluRs and/or voltage-dependent Ca^{2+} channels. QX-314 bromide salt may have inhibited Ca^{2+} entry (Talbot and Sayer 1996) and therefore prevented the detection of mGluR-mediated Ca^{2+} responses. However, in CA1 pyramidal cells mGluR-mediated depolarization and Ca^{2+} responses have been reported using such recording and stimulation protocols (Congar et al. 1997). Previous studies have reported a similar requirement for Ca^{2+} entry via iGluRs or voltage-dependent Ca^{2+} channels. Cooperative actions of either iGluRs or voltage-dependent Ca^{2+} channels along with mGluRs are necessary for oscillatory Ca^{2+} responses in OA interneurons (Carmant et al. 1997; Woodhall et al. 1999). Analogously, mGluR-mediated enhancement of synaptically evoked Ca^{2+} responses can occur via potentiation of spike-driven increases in $[\text{Ca}^{2+}]_i$ (Nakamura et al. 1999; Zheng et al. 1996). Our observation of a partial contribution of mGluRs to synaptically evoked Ca^{2+} responses with no enhancement of EPSPs or burst discharges appears contradictory to our other observation that ACPD elicited both a rise in dendritic $[\text{Ca}^{2+}]_i$ and a depolarization. The depolarization evoked by ACPD is due, however, to the activation of a Ca^{2+} -dependent cationic current (Crépel et al. 1994; McBain et al. 1994; Pozzo Miller et al. 1995; Woodhall et al. 1999). The absence of depolarization may thus be due to an insufficient elevation of $[\text{Ca}^{2+}]_i$ to activate this current following synaptic stimulation.

An important consideration in the failure to detect pharmacologically isolated synaptic mGluR responses is that the region of dendrite being imaged may not have been in the vicinity of active synapses with mGluRs. In control ACSF, synaptically evoked Ca^{2+} responses were due to activation of polysynaptic (Shaffer collaterals/pyramidal cells) and monosynaptic inputs (pyramidal cells). However, in the presence of APV and CNQX, only monosynaptic inputs were activated, which reduced the likelihood that the region of interest contained active synapses. Additionally, no action potentials contributed to synaptically evoked Ca^{2+} influx in the presence of APV and CNQX, resulting in a more spatially restricted Ca^{2+} response. Indeed, recent studies in cerebellar Purkinje neurons have demonstrated the presence of highly localized mGluR-mediated increases in dendritic $[\text{Ca}^{2+}]_i$ in response to synaptic stimulation that are not accompanied by postsynaptic currents (Finch and Augustine 1998; Takechi et al. 1998). Likewise, MCPG reduces tetanus-induced dendritic $[\text{Ca}^{2+}]_i$ rises in CA1 pyramidal neurons with little or no effect on the postsynaptic current (Frenguelli et al. 1993). The dendrites of OA interneurons lack the planar arrangement of Purkinje and pyramidal neurons, making it difficult to image much of their dendritic trees. In future experiments, it would be important to examine Ca^{2+} responses at dendritic segments with clearly identified monosynaptic excitatory inputs and activated at sub-

and supra-threshold levels. Our preliminary observation that MCPG could differentially affect synaptically evoked dendritic Ca^{2+} responses in different branches suggests that mGluR-mediated Ca^{2+} responses could be localized to certain dendritic segments in interneurons. In addition, the mechanisms for mGluR-mediated intracellular Ca^{2+} release may not be present in all parts of the dendritic tree (Berridge 1998).

Conceivably, MCPG may have directly antagonized NMDA or AMPA receptors (e.g., Contractor et al. 1998). However, our observation that MCPG did not affect burst discharges suggests that the effects on Ca^{2+} responses were not due to nonspecific antagonism of iGluRs. In disinhibited slices, antagonizing NMDA receptors reduced the number of action potentials per burst, whereas antagonism of AMPA receptors blocked burst discharges (data not shown) (Williamson and Wheal 1992). MCPG can also antagonize group II mGluRs, which have been localized to presynaptic terminals in the hippocampus (Shigemoto et al. 1997). Preventing activation of presynaptic group II mGluRs, which are negatively coupled to cAMP, is expected to enhance glutamate release during synaptic transmission (Conn and Pin 1997). MCPG did not affect synaptically evoked EPSPs and burst discharges, suggesting that there was no increase in glutamatergic transmission due to antagonism of presynaptic group II mGluRs at these synapses. Group III mGluRs are also localized presynaptically to OA interneurons (Shigemoto et al. 1996, 1997); however, MCPG does not antagonize these receptors at the concentrations used (Conn and Pin 1997). Therefore the effects of MCPG we observed were likely exerted via postsynaptic mGluRs.

Physiological implications of synaptically activated Ca^{2+} responses

Interneurons in OA and to a lesser extent in stratum pyramidale are preferentially lost in experimental models of epilepsy, whereas interneurons of stratum radiatum/lacunosum-moleculare are not (Best et al. 1993; Morin et al. 1998). While the exact mechanism of this cell loss is unknown, it likely results from seizure-induced Ca^{2+} -mediated excitotoxicity (see Dingledine et al. 1990; Meldrum 1995). Several lines of evidence suggest that the selective vulnerability of OA interneurons may be due to a Ca^{2+} -mediated mGluR mechanism. First, high levels of group I mGluRs are selectively expressed in OA interneurons (Baude et al. 1993; van Hoof et al. 2000). Second, the group I/II mGluR agonist ACPD elicits large rises in $[\text{Ca}^{2+}]_i$ in OA interneurons but not in interneurons of stratum radiatum and lacunosum-moleculare (Carmant et al. 1997; Woodhall et al. 1999). Third, in the present study we show that mGluR activation contributes in part to intracellular Ca^{2+} rises during epileptiform synaptic burst discharges. Although synaptically evoked mGluR-mediated intracellular Ca^{2+} rises are less marked than mGluR agonist-induced responses, they are likely to be more pronounced during seizure activity. It is possible that other mechanisms like Ca^{2+} influx through kainate receptors may contribute to seizure-induced excitotoxicity in OA interneurons; however, excitatory postsynaptic currents mediated by kainate are also present in interneurons of stratum radiatum and lacunosum-moleculare, which are resistant to excitotoxicity (Cossart et al. 1998; Frerking et al. 1998).

Activation of mGluRs also plays a role in long-term potentiation of excitatory synaptic transmission in OA interneurons

(Cowan et al. 1998; Ouardouz and Lacaille 1995; Perez et al. 2000; but see Maccaferri and McBain 1996). Interestingly, interneurons in strata radiatum and lacunosum-moleculare lack this form of plasticity (Ouardouz and Lacaille 1995; Perez et al. 2000). The observation that group I/II mGluR activation produces large rises in intracellular Ca^{2+} in OA interneurons but not in interneurons of strata radiatum and lacunosum-moleculare (Woodhall et al. 1999) and that group I/II mGluRs contribute in part to intracellular Ca^{2+} rises in OA interneurons during synaptic burst discharges suggest that mGluR-mediated Ca^{2+} transients may be involved in the induction of long-term potentiation at OA interneuron synapses. In other cell types, mGluRs are important for long-term potentiation (e.g., Bortolotto et al. 1999; Cohen et al. 1998; Zheng et al. 1996), particularly when long-term potentiation is induced using weak tetanization protocols that require Ca^{2+} release from internal stores (Wilsch et al. 1998).

Thus our results show that synaptic activation causes rises in dendritic $[\text{Ca}^{2+}]_i$ in OA interneurons that require ionotropic glutamate receptor activation and are mediated in part by activation of group I/II mGluR receptors. These glutamate receptor-mediated rises in $[\text{Ca}^{2+}]_i$ may have important functional implications for both normal and pathological hippocampal function.

We thank Dr. R. Robitaille for assistance with the confocal microscopy and for helpful discussions. Drs. S. Bertrand and N. Haddjeri provided critical comments on a previous version of the manuscript.

This research was supported by the Canadian Institutes of Health Research, the Fonds pour la Formation de Chercheurs et l'Aide à la Recherche (FCAR), and the Fonds de la Recherche en Santé du Québec. C. E. Gee was supported by postdoctoral fellowships from the Centre de Recherche en Sciences Neurologiques (J. P. Cordeau) and the Natural Sciences and Engineering Research Council of Canada. G. Woodhall received postdoctoral fellowships from the FCAR and Groupe de Recherche sur le Système Nerveux Central.

REFERENCES

- BAUDE A, NUSSER Z, ROBERTS JDB, MULVIHILL E, MCILHINNEY RAJ, AND SOMOGYI P. The metabotropic glutamate receptor (mGluR1 α) is concentrated at perisynaptic membrane of neuronal subpopulations as detected by immunogold reaction. *Neuron* 11: 771–787, 1993.
- BERRIDGE MJ. Neuronal calcium signaling. *Neuron* 21: 13–26, 1998.
- BEST N, MITCHELL J, AND WHEAL HV. Changes in parvalbumin-immunoreactive neurons in CA1 area of hippocampus following a kainic acid injection. *Acta Neuropathol (Berl)* 87: 187–195, 1993.
- BIANCHI R, YOUNG SR, AND WONG RK. Group I mGluR activation causes voltage-dependent and -independent Ca^{2+} rises in hippocampal pyramidal cells. *J Neurophysiol* 81: 2903–2913, 1999.
- BLASCO-IBANEZ JM AND FREUND TF. Synaptic input of horizontal interneurons in stratum oriens of hippocampal CA1 subfield: structural basis of feed-back activation. *Eur J Neurosci* 7: 2170–2180, 1995.
- BORTOLOTTI ZA, FITZJOHN SM, AND COLLINGRIDGE GL. Role of metabotropic glutamate receptors in LTP and LTD in the hippocampus. *Curr Opin Neurobiol* 9: 299–304, 1999.
- CARMANT L, WOODHALL G, OUARDOUZ M, ROBITAILLE R, AND LACAÏLLE J.-C. Interneuron-specific Ca^{2+} responses linked to metabotropic and ionotropic glutamate receptors in rat hippocampal slices. *Eur J Neurosci* 9: 1625–1635, 1997.
- CHOI DW. Calcium and excitotoxic neuronal injury. *Ann NY Acad Sci* 747: 162–171, 1994.
- COHEN AS, RAYMOND CR, AND ABRAHAM WC. Priming of long-term potentiation induced by activation of metabotropic glutamate receptors coupled to phospholipase C. *Hippocampus* 8: 160–170, 1998.
- CONGAR P, LEINEKUGEL X, BEN-ARI Y, AND CRÉPEL V. A long-lasting calcium-activated nonselective cationic current is generated by synaptic stimulation or exogenous activation of group I metabotropic glutamate receptors in CA1 pyramidal neurons. *J Neurosci* 17: 5366–5379, 1997.
- CONN PJ AND PIN J.-P. Pharmacology and functions of metabotropic glutamate receptors. *Annu Rev Pharmacol Toxicol* 37: 205–237, 1997.
- CONTRACTOR A, GEREAU RW IV, GREEN T, AND HEINEMANN SF. Direct effects of metabotropic glutamate receptor compounds on native and recombinant *N*-methyl-D-aspartate receptors. *Proc Natl Acad Sci USA* 95: 8969–8974, 1998.
- COSSART R, ESCLAPEZ M, HIRSCH JC, BERNARD C, AND BEN-ARI Y. GluR5 kainate receptor activation in interneurons increases tonic inhibition of pyramidal cells. *Nature Neurosci* 1: 470–478, 1998.
- COWAN AI, STRICKER C, REECE LJ, AND REDMAN SJ. Long-term plasticity at excitatory synapses on aspiny interneurons in area CA1 lacks synaptic specificity. *J Neurophysiol* 79: 13–20, 1998.
- CRÉPEL V, ANIKSZEJN L, BEN-ARI Y, AND HAMMOND C. Glutamate metabotropic receptors increase a Ca^{2+} -activated nonspecific cationic current in CA1 hippocampal neurons. *J Neurophysiol* 72: 1561–1569, 1994.
- DINGLEDINE R, MCBAIN CJ, AND MCNAMARA JO. Excitatory amino acid receptors in epilepsy. *Trends Pharmacol Sci* 11: 334–338, 1990.
- FINCH EA AND AUGUSTINE GJ. Local calcium signalling by inositol-1,4,5-triphosphate in Purkinje cell dendrites. *Nature* 396: 573–576, 1998.
- FRENGUELLI BG, POTIER B, SLATER NT, ALFORD S, AND COLLINGRIDGE GL. Metabotropic glutamate receptors and calcium signalling in dendrites of hippocampal CA1 neurones. *Neuropharmacology* 32: 1229–1237, 1993.
- FREKING M, MALENKA RC, AND NICOLL RA. Synaptic activation of kainate receptors on hippocampal interneurons. *Nature Neurosci* 1: 479–486, 1998.
- FREUND TF AND BUZSÁKI G. Interneurons of the hippocampus. *Hippocampus* 6: 347–470, 1996.
- GEE CE, WOODHALL G, AND LACAÏLLE J.-C. Synaptically-evoked dendritic Ca^{2+} responses in oriens-alveus interneurons of disinhibited hippocampal slices. *Soc Neurosci Abstr* 24: 1088, 1998.
- GHOSH A AND GREENBERG ME. Calcium signaling in neurons: molecular mechanisms and cellular consequences. *Science* 268: 239–247, 1995.
- LACAÏLLE J.-C, MUELLER AL, KUNKEL DD, AND SCHWARTZKROIN PA. Local circuit interactions between oriens/alveus interneurons and CA1 pyramidal cells in hippocampal slices: electrophysiology and morphology. *J Neurosci* 7: 1979–1993, 1987.
- LUJÁN R, NUSSER Z, ROBERTS DB, SHIGEMOTO R, AND SOMOGYI P. Perisynaptic location of metabotropic glutamate receptors mGluR1 and mGluR5 on dendrites and dendritic spines in the rat hippocampus. *Eur J Neurosci* 8: 1488–1500, 1996.
- MACCAFERRI G AND MCBAIN CJ. Long-term potentiation in distinct subtypes of hippocampal nonpyramidal neurons. *J Neurosci* 16: 5334–5343, 1996.
- MCBAIN CJ, DICHIARA TJ, AND KAUER JA. Activation of metabotropic glutamate receptors differentially affects two classes of hippocampal interneurons and potentiates excitatory synaptic transmission. *J Neurosci* 14: 4433–4445, 1994.
- MCBAIN CJ, FREUND TF, AND MODY I. Glutamatergic synapses onto hippocampal interneurons: precision timing without lasting plasticity. *Trends Neurosci* 22: 228–235, 1999.
- MELDRUM BS. Excitatory amino acid receptors and their role in epilepsy and cerebral ischemia. *Ann NY Acad Sci* 757: 492–505, 1995.
- MORIN F, BEAULIEU C, AND LACAÏLLE J.-C. Selective loss of GABA neurons in area CA1 of the rat hippocampus after intraventricular kainate. *Epilepsy Res* 32: 363–369, 1998.
- NAKAMURA T, BARBARA J.-G, NAKAMURA K, AND ROSS WN. Synergistic release of Ca^{2+} from IP_3 -sensitive stores evoked by synaptic activation of mGluRs paired with backpropagating action potentials. *Neuron* 24: 727–737, 1999.
- NICOLETTI F, BRUNO V, COPANI A, CASABONA G, AND KNOPFEL T. Metabotropic glutamate receptors: a new target for the therapy of neurodegenerative disorders? *Trends Neurosci* 19: 267–271, 1996.
- OUARDOUZ M AND LACAÏLLE J.-C. Mechanisms of selective long-term potentiation of excitatory synapses in stratum oriens/alveus interneurons of rat hippocampal slices. *J Neurophysiol* 73: 810–819, 1995.
- PÉREZ Y, MORIN F, AND LACAÏLLE J.-C. mGluR-mediated LTP of minimally-evoked EPSCs in hippocampal oriens interneurons induced by theta burst stimulation. *Soc Neurosci Abstr* 26: 8815, 2000.
- POZZO MILLER LD, PETROZZINO JJ, AND CONNOR JA. G protein-coupled receptors mediate a fast excitatory postsynaptic current in CA3 pyramidal neurons in hippocampal slices. *J Neurosci* 15: 8320–8330, 1995.
- SHIGEMOTO R, KINOSHITA A, WADA E, NOMURA S, OHISHI H, TAKADA M, FLOR P, NEKI A, ABE K, NAKANISHI S, AND MIZUNO N. Differential presynaptic localization of metabotropic glutamate receptor subtypes in the rat hippocampus. *J Neurosci* 17: 7503–7522, 1997.

- SHIGEMOTO R, KULIK A, ROBERTS JDB, OHISHI H, NUSSER Z, KANEKO T, AND SOMOGYI P. Target-cell-specific concentration of a metabotropic glutamate receptor in the presynaptic active zone. *Nature* 381: 523–525, 1996.
- SLOVITER RS. Decreased hippocampal inhibition and a selective loss of interneurons in experimental epilepsy. *Science* 235: 73–76, 1987.
- TAKECHI H, EILERS J, AND KONNERTH A. A new class of synaptic response involving calcium release in dendritic spines. *Nature* 396: 757–760, 1998.
- TALBOT MJ AND SAYER RJ. Intracellular QX-314 inhibits calcium currents in hippocampal CA1 pyramidal neurons. *J Neurophysiol* 76: 2120–2124, 1996.
- VAN HOOFT JA, GIUFFRIDA R, BLATOW M, AND MONYER H. Differential expression of group I metabotropic glutamate receptors in functionally distinct hippocampal interneurons. *J Neurosci* 20: 3544–3551, 2000.
- WILLIAMSON R AND WHEAL HV. The contribution of AMPA and NMDA receptors to graded bursting activity in the hippocampal CA1 region in an acute in vitro model of epilepsy. *Epilepsy Res* 12: 179–188, 1992.
- WILSCH VW, BEHNISCH T, JÄGER T, REYMANN KG, AND BALSCHUN D. When are class I metabotropic glutamate receptors necessary for long-term potentiation? *J Neurosci* 18: 6071–6080, 1998.
- WOODHALL G, GEE CE, ROBITAILLE R, AND LACAILE J-C. Membrane potential and intracellular Ca^{2+} oscillations activated by mGluRs in hippocampal stratum oriens/alveus interneurons. *J Neurophysiol* 81: 371–382, 1999.
- ZHENG F, GALLAGHER JP, AND CONNOR JA. Activation of a metabotropic excitatory amino acid receptor potentiates spike-driven calcium increases in neurons of the dorsolateral septum. *J Neurosci* 16: 6079–6088, 1996.